DIFFRACTION AT HERA

B. CLERBAUX
Université Libre de Bruxelles, CP 230, Boulevard du Triomphe,
1050 Brussels, Belgium

Recent results on diffraction from the H1 and ZEUS Collaborations are reviewed. The diffractive structure function $F_2^{D(3)}(Q^2, x_P, \beta)$ is presented, and is found to be consistent with an interpretation in which two individually factorisable components contribute, that may be identified with pomeron and meson contributions. The Q^2 and β dependences of $F_2^{D(3)}(Q^2, x_P, \beta)$ are examined in the form $F_2^{D(2)}(Q^2, \beta)$ after integrating over x_P. The t distribution is shown (t is the square of the four-momentum transfered from the virtual photon to the target). The production of D^* meson at high Q^2 is presented as an example of analysis of the diffractive final state. These analyses are consistent with a leading gluon partonic structure for the pomeron. Exclusive vector meson production is discussed, in particular J/ψ photoproduction and ϱ production at high Q^2; the data are compared to recent perturbative QCD calculations.

1 Introduction

HERA is a high energy electron (or positron) proton collider, the beam energies being respectively 27.5 GeV and 820 GeV. An important aim of the detectors H1 and ZEUS is to study the structure of the proton using the electron as a probe. An interesting class of events is thus Deep Inelastic Scattering (DIS), where the exchanged photon interacts directly with a quark inside the proton. To restore the colour neutrality of the final state hadrons, particles are created between the struck quark jet and the proton remnant jet (Fig. 1a). There exists another class of interactions: the diffractive process, which represents around 10 % of the DIS events. An interaction is called hereafter diffractive if a gap without emitted particles is observed between the dissociative photon system and the scattered proton (Fig. 1b). This means that there is no colour flow between those two systems, and the object exchanged in the $\gamma^* p$ interaction carries no colour.

In the 70's, the diffractive processes were intensively studied in hadron–hadron interactions. They are well described by the Regge phenomenology. For example the total cross–sections [a] can be parameterised using a simple

[a] The total cross–sections are linked to the elastic amplitude by the optical theorem: $\sigma_{tot} \approx s^{-1}\, ImA(el.)\ (t=0)$, s and t being defined in the text.

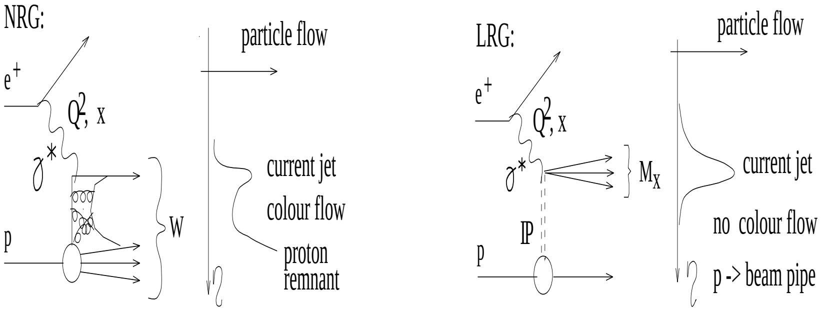

Figure 1: a) Deep Inelastic Scattering, and b) diffractive interaction.

formula with two components [1]:

$$\sigma_{tot} \;=\; as^{0.08} + bs^{-0.45}, \tag{1}$$

where s is the square of the energy in the hadron–hadron center of mass system (cms). In Regge phenomenology, the first (second) term in eq. 1 is understood as due to the exchange in the t channel of a pomeron (meson). The pomeron is an object carrying the quantum numbers of the vacuum. At high s, the exchange is dominated by the pomeron, and σ_{tot} rises slowly with energy: it is a 'soft' energy dependence of the cross–section. The interest is now to describe these interactions with the microscopic theory of the strong interaction: the Quantum Chromo–Dynamics, and in particular, to study the partonic structure of the pomeron.

The data presented here come from the H1 and ZEUS collaborations, and were taken in 1994, with a luminosity around 3 pb^{-1}, depending on the analysis. Most results are still preliminary.

2 Diffractive Structure Function

To understand diffractive interactions, one can study the diffractive cross section or equivalently the diffractive structure functions $F_2^{D(3)}(Q^2, x_P, \beta)$. Q^2 is the negative of the square of q, the 4–momentum carried by the virtual photon, and

$$x_P = q.(-k)/(q.p) \approx \frac{Q^2 + M_x^2}{Q^2 + W^2}; \quad \beta = Q^2/(2q.(-k)) \approx \frac{Q^2}{Q^2 + M_x^2}, \tag{2}$$

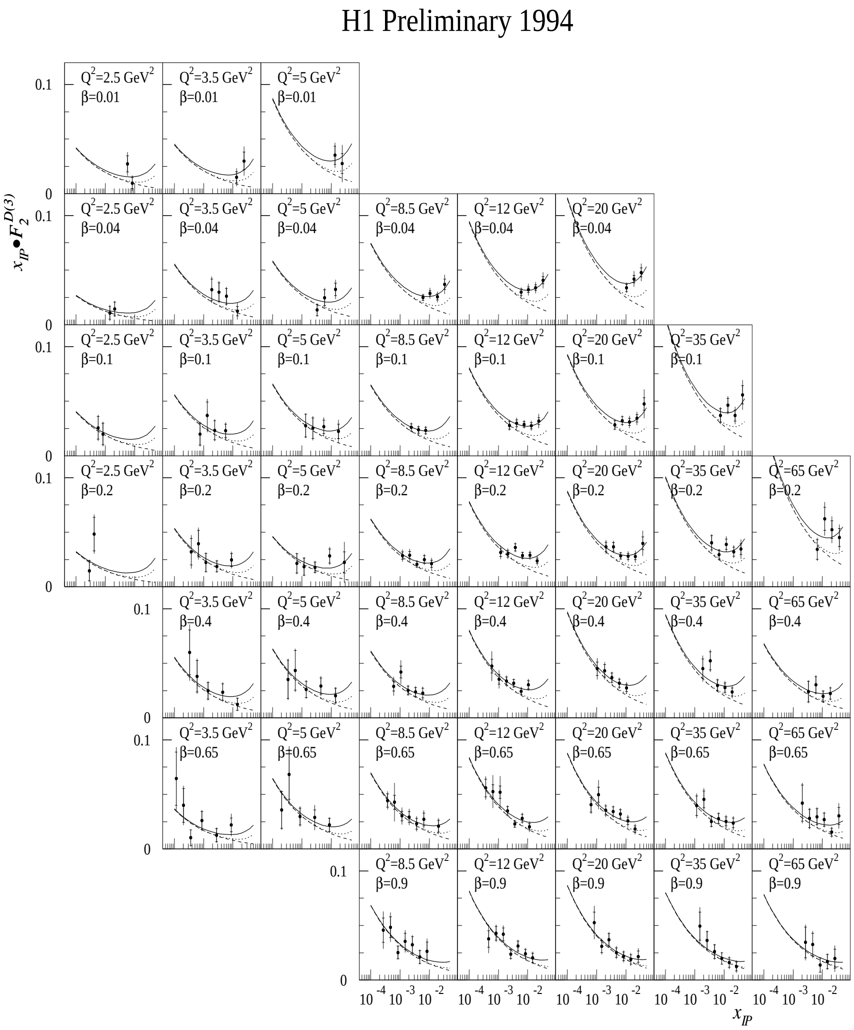

Figure 2: $x_P.F_2^{D(3)}(Q^2, x_P, \beta)$, as a function of x_P for different Q^2 and β bins (see text for the details of the fit).

where k is the 4–momentum carried by the pomeron, M_x is the invariant mass of the dissociative photon system, and W is the energy of the $\gamma^* p$ cms. For diffractive interactions, the kinematical variable $t = k^2$ is expected to be small. $F_2^{D(3)}(Q^2,\, x_P,\, \beta)$ is integrated over t. In a picture of diffractive interactions where a pomeron is emitted from the proton, the pomeron having a partonic structure, x_P is the fraction of the proton momentum carried by the pomeron, and β is the fraction of the pomeron momentum carried by the quark interacting with the virtual photon. The diffractive structure function $F_2^{D(3)}(Q^2,\, x_P,\, \beta)$ is then written as the product of two factorisable contributions: the first one describes the pomeron flux and depends only on x_P, and the second one describes the pomeron structure and depends on Q^2 and β. This decomposition applies also to the meson exchange:

$$F_2^{D(3)}(Q^2,\, x_P,\, \beta) = (1/x_P)^{n_1}.f_2^P(Q^2,\beta)+c.(1/x_P)^{n_2}.f_2^R(Q^2,\beta)+interference \tag{3}$$

In Fig. 2, the H1 1994 preliminary results [2] for $x_P.F_2^{D(3)}(Q^2,\, x_P,\, \beta)$ are presented as a function of x_P, for different Q^2 and β bins, together with a fit in which a pomeron component contributes together with a meson component, the pomeron and the meson components interfering with a relative phase of 45°. In the figure, the dashed lines show the contribution from the pure pomeron intensity, the dotted lines the sum of the pure pomeron and meson intensities, the solid lines the total contribution. For the fit, n_1, n_2, f_2^P, c are free parameters. For f_2^R, the GRV pion structure function was used. One observes that the meson exchange contribution is important at low β and large x_P. The result of the fit gives the values

$$n_1 = 1.29 \pm 0.03, \quad n_2 = 0.30 \pm 0.30; \tag{4}$$

In the Regge phenomenology, $n = 2\alpha(t) - 1$, $\alpha(t)$ describing the exchanged trajectory. n_1 is slightly higher than the value expected for a 'soft' pomeron exchange, after averaging over t, $n_1 \approx 1.08$ [b]; n_2 is consistent with the value expected for meson echange.

$F_2^{D(2)}(Q^2,\, \beta)$ is defined by integrating $F_2^{D(3)}(Q^2,\, x_P,\, \beta)$ over x_P in the range from 0.0003 to 0.05, and describes the partonic structure of the pomeron. $F_2^{D(2)}(Q^2,\, \beta)$ is presented in the Fig. 3 as a function of Q^2, for different β bins. It differs markedly from the proton structure function: $F_2^{D(2)}(Q^2,\, \beta)$ is still large at large β, and the rise with Q^2 persists to value of β much larger than $\approx$

[b] $\alpha(t) = \alpha(0) + \alpha' t$ was used, with $\alpha(0) = 1.08$, $\alpha' = 0.25$, and a mean t value of -1/6.

H1 Preliminary 1994

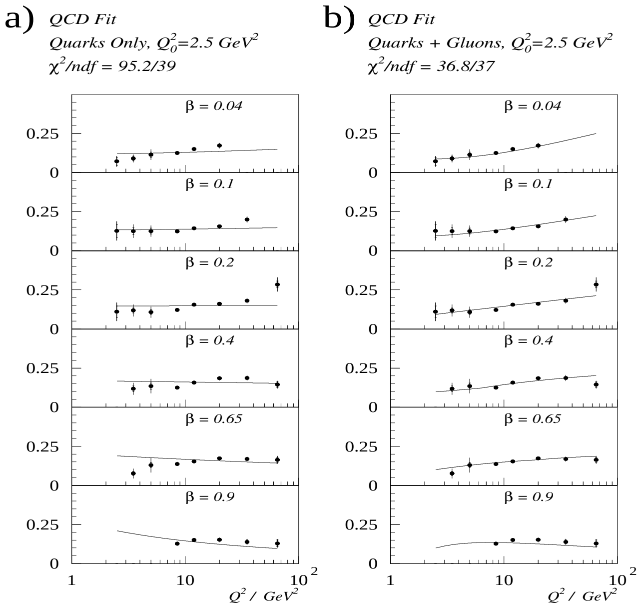

Figure 3: DGLAP QCD evolution of the (Q^2, β) dependence of $F_2^{D(2)}(Q^2, \beta)$ assuming at the starting scale of $Q_0^2 = 2.5$ GeV^2 a) quarks only, b) both quarks and gluons.

0.15. This is an indication for a dominant gluonic component in the pomeron. A QCD fit was performed on the data using the Altarelli–Parisi (DGLAP) evolution equations. Those equations let an initial parton distribution, given in function of β for a starting scale Q_0^2, evolve according to QCD as a function of Q^2. Two different initial parton distributions were considered at $Q_0^2 = 2.5$ GeV^2: only quarks, and both quarks and gluons. In the first case (see Fig. 3a), the DGLAP evolution fails to reproduce the tendency in the data for rising scaling violations at large β, whereas the mixed quark and gluon case (see Fig. 3b) is in agreement with this rise. For the latter, the corresponding parton distribution is dominated, throughout the Q^2 range, by the gluons, which carry in excess of 80 % of the momentum, this fraction decreasing slowly as Q^2 increases.

The t dependence of the diffractive cross–section can be directly measured using the Leading Proton Spectrometers (LPS), consisting of different stations situated around the proton beam pipe at distances varying from 64 to 90 m. The aim of these detectors is to identify the scattered proton and to reconstruct its momentum. Fig. 4 shows the ZEUS 1994 preliminary result [3] for the measured differential cross–section $d\sigma/d|t|$. The distribution was fitted with a single exponential form, $d\sigma/d|t| \sim \exp(-b\ |t|)$, shown as a solid line. The value of the fitted slope b is:

$$b = 5.9 \pm 1.3(stat.)\ ^{+1.1}_{-0.7}(syst.)\ \mathrm{GeV}^{-2}. \tag{5}$$

The b parameter gives information on the size of the objects participating in the interaction.

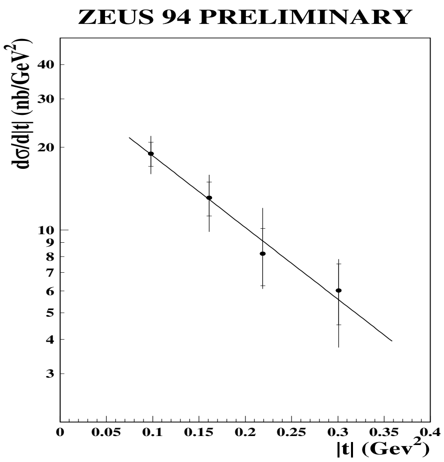

Figure 4: Differential cross–section $d\sigma/d|t|$, using the ZEUS LPS detector. The line shows the result of the exponential fit described in the text.

To understand diffraction better, one can also study the diffractive final state: jet production, hadron transverse momentum distribution, hadron energy flow, charmed particle production, etc. The analysis of these different final states is consistent with the picture of a leading gluonic component in the pomeron. For example, the H1 1994 preliminary analysis of charm production [4], gives evidence for difffractive production of D^* mesons at high Q^2 with a cross–section:

$$\sigma(ep \rightarrow eD^*XY) = 380\ ^{+150}_{-120}(stat.)\ ^{+140}_{-110}(syst.)\ pb. \tag{6}$$

The expectations from Monte–Carlo simulations with a parton distribution density as obtained from the QCD analysis of $F_2^{D(3)}$ is $\approx$ 200 pb, whereas it is, for a models with quarks only ≈ 10 pb. In the case of a mostly gluonic pomeron, the charm quark pairs can be easily produced by photon-gluon fusion, while in the quark case, charm pairs are produced in the fragmentation process and the production is therefore suppressed.

3 Exclusive measurements: Vector Meson Production

The last section concerns the diffractive production of vector mesons:

$$ep \to epV \qquad\qquad V = \varrho, \omega, \phi, J/\psi, ... \tag{7}$$

V being a meson having the same quantum numbers as the photon ($J^{PC}=1^{--}$). For these interactions, the virtual photon fluctuates into a quark–antiquark pair, which exchanges 4–momentum with the proton in order to create a real vector meson. This 4–momentum exchange is carried by the pomeron. These exclusive processes are interesting because predictions exist, based on either perturbative or non–pertubative QCD calculations. In both cases, the pomeron is modelled as a two gluons system. In the case of predictions based on perturbative QCD, a hard scale is needed, which can be either high Q^2, high quark mass (for the J/ψ), or high t, and the cross–section is expected to be proportional to the square of the gluon density in the proton; the energy dependence of the cross–section is then 'hard', i.e. rises fast with the energy. In the case of non–perturbative QCD models, the energy dependence of the cross–section is 'soft': the cross–section rises slowly, similarly to the hadron-hadron cross–section.

A compilation of results on the W dependence of the cross–section for ϱ, ω, ϕ, J/ψ vector meson production as well as for the total γp cross–section is presented in Fig. 5 for $Q^2 \approx 0$ GeV^2 (photoproduction). The cross–section is observed to rise slowly with energy for ϱ, ω, ϕ production (soft behaviour). The dependence is found to be much 'harder' for the J/ψ production.

For J/ψ photoproduction, pertubative QCD calculations have been performed using the charm quark mass as a hard scale. In Fig. 6, the J/ψ data [5] are compared with predictions [9] for different parton density distributions in the proton. Because of a sizeable normalisation uncertainty, the shape of the predicted cross–section is the best descriminator. The MRS(G) parton distribution seems to be ruled out.

Several perturbative QCD predictions exist concerning ϱ production, the high Q^2 providing a hard scale. The ϱ cross–section as a function of x is shown

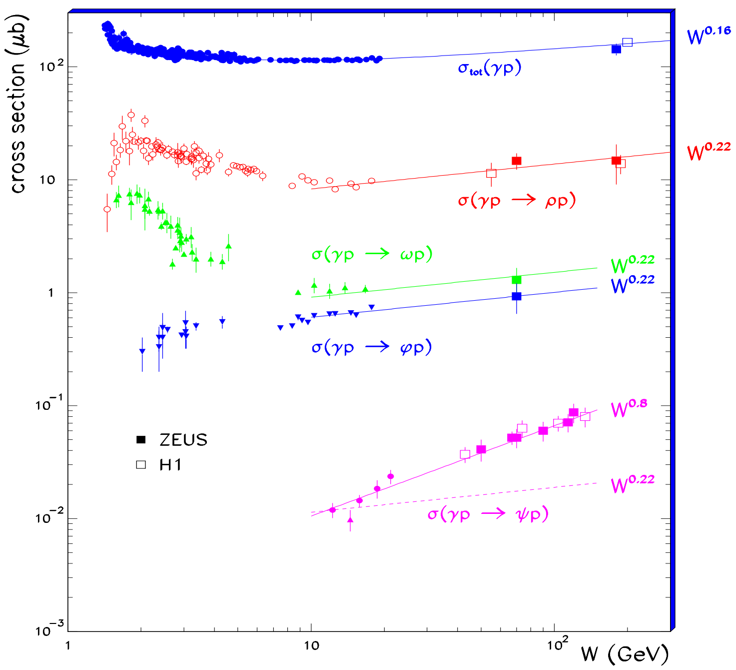

Figure 5: Compilation of results on the W dependence of the cross–section for the ϱ, ω, ϕ, J/ψ vector meson production, together with the W dependence of the total γp cross–section. The data come from H1, ZEUS and lower energy experiments.

in Fig. 7, divided in four Q^2 bins [6]; x is the Bjorken scaling variable: $x \approx Q^2/(W^2+Q^2)$. On the Figure, the full lines are from calculations [10] for different parton distributions in the proton. At high Q^2, the shape of the data seems to be well reproduced by theory. However for the lower Q^2 bins, the cross–section behaviour is flatter and compatible with a soft dependence. With more statistics, the W dependence of the cross–section will be an interesting way to study the transition between soft and hard physics in diffractive phenomena.

In 1995 a new electromagnetic calorimeter covering positron scattering angles between 17 and 35 mrad was installed into the ZEUS detector. It allows the study of ϱ production for Q^2 between 0.25 and 0.85 GeV^2. For an average Q^2 of 0.48 GeV^2, the ZEUS 1995 preliminary analysis found a cross–section that grows with increasing W at a rate consistent with that observed in photoproduction [7]. The ZEUS Collaboration has also presented

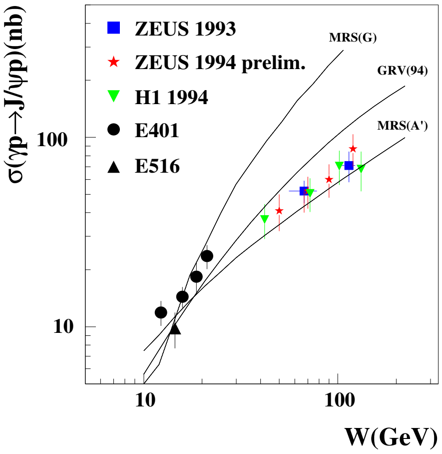

Figure 6: Exclusive J/ψ photoproduction cross–section, as a function of W. The data come from H1, ZEUS and lower energy experiments. The results of pQCD calculations are shown for various choices of parton distributions in the proton.

1995 preliminary results on the mass spectrum and the angular distribution for the two–pion diffractive photoproduction in the ϱ region at large $|t|$[8]. Also in this domain, the two–pion mass spectrum exhibits a dominant resonant contribution, and the ϱ mesons have a helicity ± 1.

4 Conclusions

The analysis of the diffractive structure functions sheds light on the nature of the diffractive interaction, which can be understood as due to the exchange of a pomeron consisting mostly of gluons. The results concerning diffractive final states support this idea. For the exclusive vector meson production, different QCD calculations can be tested, in particular for J/ψ photoproduction and for high Q^2 ϱ production. This channel can also provide information on the transition between the soft and the hard regime.

Acknowledgments

I thank the Canadian Institute for Theoretical Astrophysics (CITA) for support for attendance.

1994 ZEUS preliminary

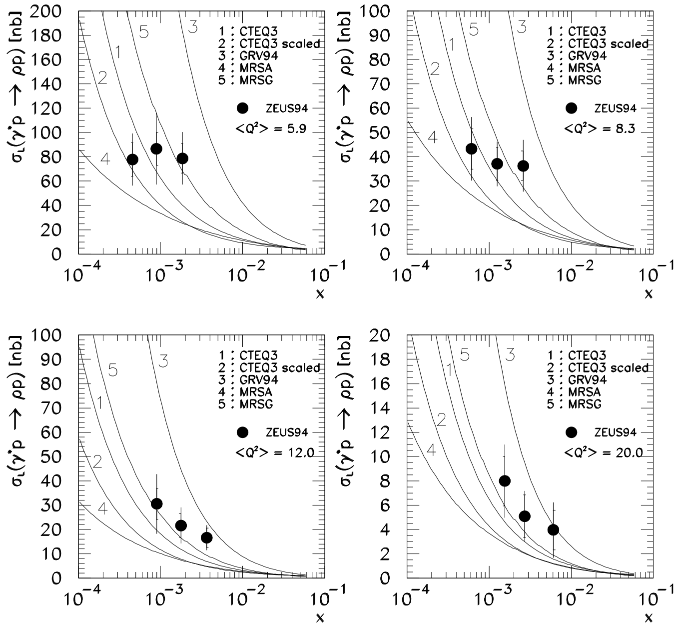

Figure 7: Exclusive ϱ production cross–section, as a function of x. The data are compared to pQCD calculations. The theoretical uncertainty is about 30 %. The normalistaion uncertainty on the data is about 15 %.

References

1. A. Donnachie, P.V. Landshoff, *Phys. Lett.* B296(1992)227.

Contributions to the 28th International Conference on High Energy Physics, 25-31 July 1996, Warsaw, Poland:

2. H1 Coll. pa02-061.
3. ZEUS Coll. pa02-026.
4. H1 Coll. pa02-060.
5. H1 Coll. pa02-085, ZEUS Coll. pa02-047.
6. ZEUS Coll. pa02-028.
7. ZEUS Coll. pa02-053.
8. ZEUS Coll. pa02-051.

9. M.G. Ryskin *et al.*, RAL-TR-95-065.
10. L. Frankfurt *et al.*, *Phys. Rev.* D54(1996)3194